Integrity assessment of corroded pipelines using dynamic segmentation and clustering

Rafael Amaya-Gómez, Mauricio Sánchez-Silva, Felipe Muñoz

Version of Record: https://www.sciencedirect.com/science/article/pii/S0957582018307870
Manuscript_5139079553a98d251fac61a95307069e

Integrity assessment of corroded pipelines using dynamic segmentation and clustering

Rafael Amaya-Gómez[a,c,*], Mauricio Sánchez-Silva[b], Felipe Muñoz[a]

[a] *Chemical Engineering Department, Universidad de los Andes, Cra 1E No. 19A-40, Bogotá, Colombia*
[b] *Department of Civil & Environmental Engineering, Universidad de los Andes, Cra 1E No. 19A-40, Bogotá, Colombia*
[c] *Université de Nantes, GeM, Institute for Research in Civil and Mechanical Engineering, CNRS UMR 6183, Nantes, France*

Abstract

Corrosion defects impact the resistance of hydrocarbon pipelines by increasing the risk of failure and the resulting Loss of Containment (LOC). Different approaches have been proposed to estimate this risk of failure based on empirical approaches (e.g., API 579-1/ASME FFS-1, ASME B318S or API1160), and other focus on probabilistic evaluations. Nevertheless, few works are dealing with spatial variability of corrosion defects and how segmentation (required for reliability evaluation) may affect intervention decisions. In this paper, information obtained from In-Line Inspections (ILI) is used to build a corrosion degradation model under a pressure-stress failure criterion, which is used in turn, to develop a dynamic segmentation strategy. This strategy aims at identifying optimal intervention times and Locations. Results show that existing reliability evaluations using static segmentations are suboptimal and may hide critical zones. This result is illustrated by a real case study in which corrosion evolution is better estimated, and the problems associated with conventional static segmentation are stressed.

Keywords: Corrosion, Dynamic Segmentation, Pipeline Integrity, In-Line Inspections, Clustering.

1. Introduction

1.1. Pipeline integrity

Pipeline integrity comprises concepts of failure prevention, inspection-repair strategies, and products, practices, and services that help operators maximize assets lifetime. According to Kishawy & Gabbar (2010), an integrity management program has eight main components out of which four of them are of particular interest in this study: i) a process to identify pipeline segments and their failure modes; ii) repair/replacement criteria ; iii) a continual process of assessment and evaluation to maintain the pipeline integrity; and iv) a process for the review of integrity assessment results. These components are related to pipeline risk management and aim to extend the pipeline lifetime based on integrity evaluation results. To this end, several approaches have been proposed to evaluate pipeline integrity including standards such as API

*Corresponding author, Tel. (+57-1) 3394949 Ext.3095
Email address: r.amaya29@uniandes.edu.co (Rafael Amaya-Gómez)

579-1/ASME FFS-1 (*Fitness-For-Service*), ASME B318S (*Managing System Integrity of Gas Pipelines*) or API1160 (*Managing system integrity for hazardous liquid pipelines*); Finite Elements Modeling (FEM) (Berstad et al., 2011; Varga & Fekete, 2017); structural evaluations based on a failure assessment diagram (Adib-Ramezani et al., 2006); and probabilistic/stochastic integrity assessments (Amaya-Gómez et al., 2018, 2016).

1.2. Corrosion

Corrosion is one of the main pipeline degradation mechanisms and a top objective of integrity management. It is a progressive degradation process associated with continuous increments of metal loss, which can be determined through In-Line (ILI) inspections. These inspections provide information about defect length, width, and depth to evaluate pipeline integrity at a given time based on phenomenological (Tang et al., 2009; Zhang et al., 2013), simulation (Caleyo et al., 2009; Li et al., 2009), or empirical approaches (de Waard & Lotz, 1993; NACE International, 2002; NORSOK, 1998). The main challenge of a corrosion assessment is to make predictions of the pipeline condition between scheduled inspections (i.e., every 2 to 6 years apart). In this direction, some approaches are using random variable adjustments (Amaya-Gómez et al., 2016; Pandey & Lu, 2013) and stochastic processes (Amaya-Gómez et al., 2018; Zhang & Zhou, 2014) to predict depth increments based on several inspections. For instance, if there are m detected defects and n ILI measurements, the depth increment δ_j^i of the *i-th* defect in the *j-th* inspection could be obtained by:

$$\begin{aligned} \Delta_x &= \{\delta_j^1, \ldots, \delta_j^m\} \quad \forall\, j \in 2, 3, \ldots, n \\ \Delta_x &= \left\{(x_j^1 - x_{j-1}^1), \ldots, (x_j^m - x_{j-1}^m)\right\} \quad \forall\, j \in 2, 3, \ldots, n, \end{aligned} \tag{1}$$

where x_j^i denotes the depth of the *i-th* defect at the *j-th* ILI measurement. These increments are used to fit a given distribution or continuous stochastic process.

1.3. Corroded pipeline integrity management

Pipeline integrity management is a performance-based process that handles pipeline serviceability and failure prevention considering the hazardousness of the transported materials. This process includes pipeline inspection, integrity assessment, and pipeline maintenance. Pipeline inspections aim to detect anomalies such as corrosion defects, cracks, or dents through direct assessments, hydrostatic tests or ILI inspections. Integrity assessments seek to evaluate the reliability-based condition of the defects. Finally, maintenance approaches propose intervention policies to assure pipeline serviceability and a lifetime extension. Some available approaches for corroded pipelines are described below.

ILI measurements are the main testing procedure used to follow corrosion evolution. ILI tests provide valuable geometric and localized information of the defects identified along the pipeline using tools such as MFL (Magnetic Flux Leakage) and UT (Ultrasonic). The MFL consists of a magnetic flux induced on the pipe wall, which leaks out when the PIG (Pipeline Inspection Gauge) find an anomaly on the pipe. The UT uses the reflexion time and the angle of ultrasound waves to detect the metal loss. The information obtained from these tools is commonly used to determine the pipeline condition (Wang et al., 2015a; Zhang & Zhou, 2014).

Based on these ILI inspections, the metal loss can be assessed by several approaches following empirical, numerical or probabilistic models. Among the empirical approaches, McAllister

(2014) presents a complete description of methods to address the problem of corrosion and coatings in pipelines. ASME B31G illustrates a manual to determine the remaining strength of a corroded pipeline (ASME, 2009). Moreover, standards such as the API 579-1/ASME FFS-1 and BS 7910 are generic fitness-for-purpose to assess how significant are defects in a range of structures empirically. Numerical approaches to assess pipeline condition usually deal with Finite Elements simulations to determine ductile failure (Varga & Fekete, 2017). Finally, available probabilistic approaches evaluate plastic collapse, yielding, or leak failure criteria (Ahammed & Melchers, 1997; Amaya-Gómez et al., 2016; Amirat et al., 2006; Hasan et al., 2012; Kale et al., 2004). The plastic collapse is evaluated through burst pressure approaches like ASME B31G, DNV RP-F101, CSA Z662 or the model proposed by Netto (Netto et al., 2005; Teixeira et al., 2008). Yielding criteria can be described based on longitudinal and circumferential stresses included in a Von Mises approach (Amirat et al., 2006). A leak failure criterion is based on a critical defect-depth, which is commonly taken as 85% of the pipeline wall thickness (Kale et al., 2004). Overall, these failure criteria are assessed through safety margins –or limit states– using operating or mechanical parameters to estimate pipeline failure probability. Nevertheless, to support maintenance decisions, critical segments have to be identified along the pipeline; hence spatial variability of the pipeline condition or soil properties have to be considered in how these segments are defined (Sahraoui & Chateauneuf, 2016).

Segmentation is the process of defining pipe sectors with similar characteristics (external or internal) that can be used as units for integrity evaluation. Segmentation can be static – i.e., initially predefined–, or dynamic - i.e., adaptable to mechanical or external conditions. Static segmentations use fixed distances defined arbitrarily (e.g., one mile) or it is defined by specific mechanical elements of particular interest such as valves. In static segmentation, there is considerable variability in the results of risk assessment and may increase intervention costs due to unnecessary evaluations. Furthermore, critical zones can be hidden if risks are weighted throughout long segments. In the dynamic segmentation, the length is not relevant as long the feature on which the segmentation is evaluated remain constant throughout the entire segment (Muhlbauer, 2004). From these two approaches, static segmentations are commonly implemented; some examples of integrity evaluations based on static segmentation can be found in Ahammed & Melchers (1997); Amirat et al. (2006); Hasan et al. (2012); Teixeira et al. (2008). However, a dynamic segmentation seems to be more reasonable for corroded pipelines, where localized defects are common along the pipeline.

Finally, the results of an ILI inspection are central to define a condition-based maintenance policy. Many approaches have been proposed in this direction for corroded pipelines (Gomes & Beck, 2014; Sahraoui et al., 2013; Zhang & Zhou, 2014). Zhang & Zhou (2014) presented a cost-based maintenance policy using costs of inspection, excavation, repair, and failure replacement representative of the typical industry practice in Canada for corroding natural gas pipelines. Gomes & Beck (2014) exposed a cost-based model to determine an optimal corrosion thickness, time-to-first inspection, and time between successive inspections. These approaches seek to minimize total expected life-cycle costs, i.e., costs of construction, inspections, repair, and expected loss.

1.4. Objective and paper structure

The objective of this paper is to identify critical segments along the pipeline based on modern degradation methods and dynamic segmentation. Dynamic segmentation depends upon the assessment criteria; in this paper, it will be defined for the particular case of corrosion integrity based on information from ILI inspections. The document is structured as follows: Section 2

describes the proposed pipeline integrity evaluation. Section 3 describes the case study, and the results and discussion are shown in Section 4. Finally, conclusions are given in Section 5.

2. Pipeline integrity evaluation

2.1. Overview

The proposed methodology follows three phases. First, a stochastic corrosion degradation process is used based on data collected and processed from ILI measurements. In this paper, the corrosion is modeled by a Mixed-Lévy approach, based on the results from a previous work (Amaya-Gómez et al., 2018). This approach uses a Gamma Process (GP) and a Compound Poisson process (CPP) with shocks distributed as Delta-Dirac in a linear combination of their constitutive processes. Second, a reliability assessment approach based on pipeline failure probability, dynamic segmentation, and the definition of a critical region is proposed. Finally, critical segments are identified based on recognized threshold evaluations and the results from the critical region.

2.2. Reliability assessment approach

In engineering design, the distinction between failure and safe condition is typically defined in terms of a limit state function $g(\mathbf{X})$ (Sánchez-Silva & Klutke, 2016). Several failure mechanisms can be formulated for pipelines such as a plastic collapse, yielding, or leak. A plastic collapse considers a pressure-based limit state (i.e., $g_P = P_b - P_{op}$) between the pipeline burst pressure (P_b), in which the pipe wall will bulge outward and reach a point of instability, and the pipeline operating pressure (P_{op}). A yielding failure uses a stress limit state (i.e., $g_S = \sigma_Y - \sigma_{Equiv}$), which includes longitudinal and circumferential stress loads that can be evaluated with equivalent stresses like Von Mises or Tresca. Finally, leaks are based on the consumption of the wall thickness (i.e., $g_D = d_c - d$) and predefined critical depth are used for this purpose as resistance. These failure criteria can be implemented separately to support intervention decisions, but in this paper, the pressure and the stress failure criteria are considered jointly for illustrative purposes. The latter with the aim to evaluate a somehow conservative failure criterion by following an isotropic material at which the Von Mises stress is compared to the pipeline ultimate strength, as it was previously implemented in some FEM simulations like Andrade & Benjamin (2004). The combined approach is developed based on the models reported by Netto et al. (2005) and Amirat et al. (2006), which are described below.

2.2.1. Pressure failure criterion

Netto et al. (2005) proposed a model to calculate the burst pressure of moderate-to-high toughness pipes (API 5L X52 to X77) assuming that the corrosion defects have ideal elliptical shapes. Based on a set of low-scale experiments and non-linear numerical finite elements simulations, both for an intact and a corroded pipeline, they obtained the following limit state:

$$g_P = \left[\frac{(1.1\sigma_y)2t}{D}\right]\left[1 - 0.9435\left(\frac{d}{t}\right)^{1.6}\left(\frac{l}{D}\right)^{0.4}\right] - P_{op}, \tag{2}$$

where σ_y is the yield strength, D is the diameter, t is the wall thickness, d is the defect-depth, and l is the defect length. This approach was chosen because it produces less conservative predictions than other recognize models such as ASME B31G, DNV RP-F101, and CSA Z662-07 (Amaya-Gómez et al., 2019; Amaya-Gómez et al., 2016; Hasan et al., 2012; Teixeira et al., 2008).

2.2.2. Stress failure criterion

Amirat et al. (2006) used a model based on longitudinal and circumferential stresses previously described by Ahammed & Melchers (1997). Longitudinal stresses depend on the load and support conditions throughout the pipeline, whereas circumferential stresses on the transversal propagation of the applied load at the top of the pipeline and the propagation as a reaction at the bottom (Ahammed & Melchers, 1997). They used the failure criterion of energy distortion theory, which according to Ahammed & Melchers (1997), has obtained acceptable results compared to other experimental approaches for ductile materials. The limit state function is expressed in terms of longitudinal and circumferential stresses as follows:

$$g_S = \sigma_y - \sigma_{Equiv} = \sigma_y - \sqrt{\sigma_c^2 - \sigma_c \sigma_l + \sigma_l^2}, \tag{3}$$

where σ_{Equiv} is the Von Mises equivalent stress.

The circumferential and longitudinal stresses are given by:

$$\begin{aligned} \sigma_c &= \sigma_{Pc} + \sigma_{Sc} + \sigma_{Tc} + \sigma_{Resc}, \\ \sigma_l &= \sigma_{Pl} + \sigma_{Sl} + \sigma_{Tl} + \sigma_{Resl}, \end{aligned} \tag{4}$$

where σ_{Pc} is the inner pressure stress, σ_{Sc} is the circumferential bending stress due to overlaying soil, σ_{Tc} is the traffic load, σ_{Pl} is the tensile stress, σ_{Sl} is the thermal stress, σ_{Tl} is the external bending load, and σ_{Resc}, and σ_{Resl} are the residual stresses. Overall, σ_{Pc} and σ_{Pl} are stresses due to internal pressure; σ_{Sc} and σ_{Sl} to soil loading; and σ_{Tc} and σ_{Tl} to bending stresses (Amirat et al., 2006). Table 1 summarizes these expressions, which are explained in detail by Ahammed & Melchers (1997).

Table 1: Longitudinal and Circumferential Stress expressions (Ahammed & Melchers, 1997)

Stress cause	Longitudinal	Circumferential	Variables description
Internal pressure	$\sigma_{Pl} = \frac{\mu P r}{t}$	$\sigma_{Pc} = \frac{P r}{t}$	Poisson's ratio (μ), internal pressure (P), internal radius (r), and wall thickness (t).
Soil Loadings	$\sigma_{Sl} = \alpha E \Delta\theta$	$\sigma_{Sc} = \frac{6k_m C_d \gamma B_d^2 E t r}{E t^3 + 24k_d P r^3}$	Thermal expansion coefficient (α), elasticity modulus (E), temperature variation ($\Delta\theta$), width of the ditch (B_d), coefficient of earth pressure (C_d), bending coefficient (k_m), soil density (γ), and deflection coefficient (k_d).
Bending	$\sigma_{Tl} = E r \chi$	$\sigma_{Tc} = \frac{6k_m I_c C_t F E t r}{L_e(E t^3 + 24k_d P r^3)}$	Longitudinal curvature (χ), impact factor (I_c), surface load coefficient (C_t), surface wheel load (F), and effective pipe length (L_e).

This model contemplates residual effects that are commonly found inside materials due to construction, thermal, and mechanical/heat formation processes. Residual stresses are generated in hot lamination processes, which introduce a significant deformation for pipelines (Amirat et al., 2004). The approach from Amirat and co-workers contemplates the Crampton model, which approximates residual circumferential stresses for thin pipelines by cutting on the complete system and measuring changes of its diameter. These stresses are relaxed in corroded pipelines due to a redistribution throughout the pipeline remaining wall thickness. Thus, this model can be expressed in terms of the corroded layer t_c, wall thickness t, and radial coordinate r_t as follows (Amirat et al., 2006):

$$\sigma_{Resc} = -70\left(1 - \frac{2t_c}{t}\right)\left(1 - \frac{2(r_t - t_c)}{t - t_c}\right). \tag{5}$$

The longitudinal residual stress is determined with the Poisson coefficient μ and the circumferential stress σ_{Resc} by $\sigma_{Resl} = \mu\,\sigma_{Resc}$.

Once the limit state function g is defined (e.g., $g = g_S$ or $g = g_P$), the failure probability can be computed based on the so-called generalized reliability equation, which can be expressed as follows:

$$R = \mathbb{P}[g(\mathbf{X}) > 0] = \int \cdots \int_{g(\mathbf{X})>0} f_{\mathbf{X}}(\mathbf{x}) d\mathbf{x}, \tag{6}$$

where $f_{\mathbf{X}}$ is the joint probability density function of the n- dimensional vector $\mathbf{X}$ of basic variables that describe the problem (Sánchez-Silva & Klutke, 2016). Thus, based on the operating conditions and the material properties (i.e., operating pressure and material strength), it is possible to determine the probability that the pipeline is in a safe ($g > 0$) or in a failure ($g \leq 0$) state by computing its reliability $R = \mathbb{P}[g(\mathbf{X}) > 0]$. The complexity of this calculation depends on the number of random variables and the form of the limit state function. Then, only in a few cases Eq. 6 has an analytical solution, so alternative solution methods such as FORM/SORM or Monte Carlo simulations should be considered instead. In this paper, Monte Carlo simulations are used following a combined failure criterion described in the next section.

2.2.3. Combined failure probability approach

Although the stress approach includes loads to support the inner fluid pressure, the pressure and stress failure criteria are considered as independent events. The combined failure approach is estimated by the union of these two events, i.e., $\mathbb{P}(\mathcal{A} \cup \mathcal{B}) = \mathbb{P}(\mathcal{A}) + \mathbb{P}(\mathcal{B}) - \mathbb{P}(\mathcal{A} \cap \mathcal{B})$. Where $\mathcal{A}$ corresponds to the pressure failure event and $\mathcal{B}$ is the stress failure event. The failure approach based on the probability of the two events is described in more detail in Algorithm 1.

Algorithm 1 Combined Failure Probability (Monte Carlo Simulation)

Input: N (Iterations), T (Evaluating years) and data to estimate both Failure Probabilities (See Sections 2.2.1 and 2.2.2).
Procedure: Combined P_f

1: **for** $i = 1$ to T **do**
2: Determine the Corrosion rate and defects' depth for the i^{th} year (See Section 1.2).
3: **for** $j = 1$ to N **do**
4: Evaluate the Pressure (g_P) and Stress (g_S) limit state functions using the Inverse Sampling Method.
5: **end for**
6: Calculate: $I_P = \#(g_P \leq 0)$, $I_S = \#(g_S \leq 0)$, and $I_C = \#(g_P \leq 0 \wedge g_S \leq 0)$ {Where #(< *condition* >) is the number of cases that satisfies the condition.}
7: Calculate the combined P_f for the i^{th} year for every defect: $P_{f_i} = \dfrac{I_P + I_S - I_C}{N}$
8: **end for**
9: Determine the mean Failure Probability of the reported defects.

2.2.4. Dynamic Segmentation and Critical region

Consider a fix segment length d_{seg} in which the pipeline length L_p can be divided into $n = L_p/d_{seg}$ segments. The failure probability of every segment is determined following the combined approach mentioned in Section 2.2.3. Once this task is carried out, segments are shifted a distance $\Delta d_{seg} < d_{seg}$; i.e., $\Delta d_{seg} = \zeta \cdot d_{seg}$, where for example $\zeta \approx 0.1$, and the failure probability is recalculated. Segments are shifted until they reach the location of an original segment; i.e., k times with $k = d_{seg}/\Delta d_{seg}$. Once the segment has been shifted k times and the failure probabilities are calculated, the largest and shortest probabilities are used in a secant interpolation approach

to determine upper and lower envelopes (Fig. 1). For this purpose the *env_secant* and *smooth1q* Matlab®functions developed by Martin (2010) and Garcia (2014) are implemented.

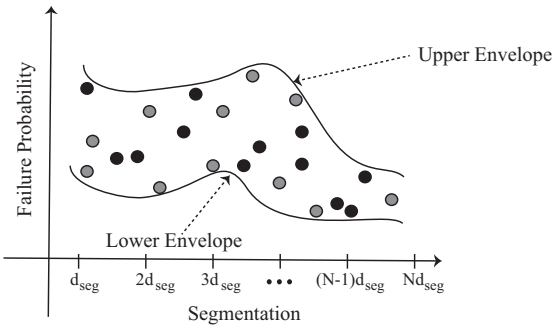

Figure 1: Dynamic Segmentation Scheme-Upper Envelope

Segment length d_{seg} is determined by maximizing the mean difference between the failure probability without segmentation ($P_{f_{NS}}$) and both envelopes for a given segment length $\mathcal{I}$:

$$\max_{\mathcal{I}\in\mathcal{S}} \frac{\alpha_U}{N}\sum_{j=1}^{N}\left|\mathcal{E}_U^j(\mathcal{I}) - P_{f_{NS}}\right| + \frac{\alpha_L}{N}\sum_{j=1}^{N}\left|\mathcal{E}_L^j(\mathcal{I}) - P_{f_{NS}}\right|, \tag{7}$$

where $\alpha_U = 0.5$ and $\alpha_L = 0.5$ are two superposition coefficients and $\mathcal{S}$ is the set of possible segment lengths such that $\max(\mathcal{S}) = \overline{\delta} < L_p$. Considering the entire joint replacement recommendation in case of a corrosion failure (ERCB, 2011), $\min(\mathcal{S}) = \underline{\delta} \geq \upsilon$ where υ is the minimum reported joint length of the pipeline. Algorithm 2 illustrates how this segment length is determined per evaluating year.

Algorithm 2 Length Segment Determination/evaluating year

Input: Δd_{seg} and data to determine the combined Failure Probability (See Section 2.2.3).
Procedure: d_{seg} {Fix segment length}
1: Calculate $P_{f_{NS}}$ {See Algorithm 1}.
2: **for** $j = \underline{\delta}$ to $\overline{\delta}$ **do**
3: Set $d_s = j$, $n = \left\lceil L_p/d_s \right\rceil$ and $k = d_s/\Delta d_{seg}$. Calculate P_f of each segment: $[d_s(\gamma-1), d_s\gamma], \forall\gamma = 1, 2, \ldots, n$. {Where $\lceil\cdot\rceil$ is the ceiling function}
4: **for** $i = 1$ to k **do**
5: Calculate P_f of each segment: $\left[(d_s + i\Delta d_{seg})(\gamma-1), (d_s + i\Delta d_{seg})\gamma\right], \forall\gamma = 1, 2, \ldots, n$.
6: **end for**
7: Determine upper ($\mathcal{E}_U(d_s)$) and lower ($\mathcal{E}_L(d_s)$) envelopes with the secant interpolating method {See (Martin, 2010)}
8: Calculate for each defect ($l = 1, \ldots, N$): $\Delta_U^l = \left|\mathcal{E}_U^l(d_s) - P_{f_{NS}}\right|$ and $\Delta_L^l = \left|\mathcal{E}_L^l(d_s) - P_{f_{NS}}\right|$.
9: Calculate: $dEval_j = \alpha_U \sum_{l=1}^{N} \Delta_U^l + \alpha_L \sum_{l=1}^{N} \Delta_L^l$
10: **end for**
11: Calculate: $d_{seg} = \max_{\underline{\delta}\leq j\leq\overline{\delta}} dEval_j$.

Based on these length segments for each evaluating year, a critical region is proposed for a spatial/temporal evaluation. This critical region is obtained from the upper/lower envelopes quartiles, i.e., 25, 50 and 75% of the data. Then, three critical temporal regions are proposed to illustrate the pipeline condition along the entire abscissa.

2.3. Pipeline integrity

The pipeline integrity is assessed by identifying critical segments based on a dynamic segmentation, which in turn, is evaluated considering the possibility of observing "corrosion colonies" and how they may cluster depending on the closeness of defects. The cluster-based assessment takes into account the fact that these colonies (which will be named as a group) require lower pressure loads for a burst failure than when evaluated them individually (Benjamin et al., 2016).

2.3.1. Grouping criterion

There are several grouping criteria between adjacent corrosion defects on pipelines such as the standards: DNV RP F-101, BS 7910, CSA Z184, ASME B31G or API 579-1/ASME FFS-1. Moreover, grouping criteria based on a limit distance between defects either circumferentially or longitudinally are also commonly used (Benjamin et al., 2007). Some of the most recognized criteria are shown in Table 2.

Table 2: Corrosion defects-grouping criteria (Benjamin et al., 2007).

Approach	Defect Grouping criterion	Longitudinally limit	Circumferentially limit
DNV RP-F101	$s_L \leq s^L_{lim}$ & $s_c \leq s^c_{lim}$	$s^L_{lim} = 2\sqrt{D\,t}$	$s^c_{lim} = \pi\sqrt{t\,D}$
Kiefner & Vieth	$s_L \leq s^L_{lim}$ & $s_c \leq s^c_{lim}$	$s^L_{lim} = 25.4mm$	$s^c_{lim} = 6t$
POF	$s_L \leq s^L_{lim}$ & $s_c \leq s^c_{lim}$	$s^L_{lim} = \min(6t, L_1, L_2)$	$s^c_{lim} = \min(6t, w_1, w_2)$
ASME B31G	$s_L \leq s^L_{lim}$ & $s_c \leq s^c_{lim}$	$s^L_{lim} = 3t$	$s^c_{lim} = 3t$

From the approaches shown in Table 2, DNV RP-F101 and ASME B31G represent attractive alternatives to calculate burst pressure of grouped defects. They obtained errors close to 5% and 23% in experimental results (Benjamin et al., 2007). Other criteria that have relevant experimental results are the so-called MTI (Mixed-Type Interaction), which is a particular case of the DNV criterion, and the grouping criterion from API 579-1/ASME FFS-1 (Benjamin et al., 2007). The API 579-1/ASME FFS-1 criterion uses an imaginary box based on the twice of the defect extent (i.e., $2s, 2c$) to cluster defects included in this rectangular section (API, 2007). In this work, the grouping criteria from DNV RP-F101, API 579-1/ASME FFS-1, and ASME B31G are compared.

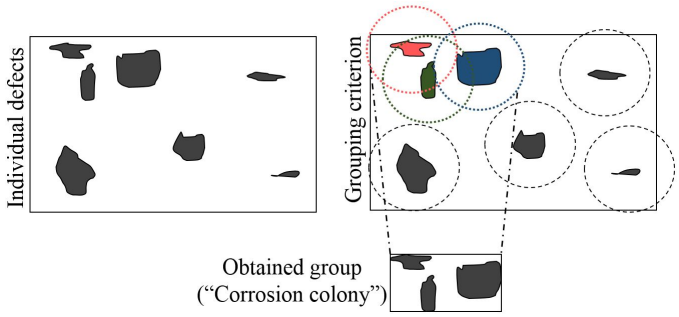

Figure 2: Equivalent corrosion colony dimensions. Adapted from Amaya-Gómez et al. (2016)

Besides, two synthetic learning approaches are also evaluated: i) k-nearest neighbor algorithm (KNN) using a Euclidean distance and k=1 with K-means (KM) with 8085 corrosion

groups, and ii) a K-means stand-alone approach with 8000 corrosion groups. Further details about these approaches were described by Amaya-Gómez et al. (2016). Both standards and the synthetic learning criteria aim to generate equivalent dimensions of the grouped defects (i.e., "corrosion colonies") using an enveloping rectangle that covers them as shown in Fig. 2.

2.3.2. Critical segments identification

This approach seeks to determine: i) when should be intervened the pipeline, ii) where these interventions should be addressed, and iii) which corrosion groups have critical failure probabilities. For this purpose, the recognized safety thresholds reported by DNV RP-F101 are considered to determine non-acceptable segments along the pipeline. These thresholds depend on annual failure probability as follows: i) $< 10^{-5}$ (High Level), ii) $< 10^{-4}$ (Normal Level) and iii) $< 10^{-3}$ (Low Level) (DNV, 2010). Fig. 3 illustrates how works the proposed approach. Initially, the time to intervene the pipeline is estimated using the failure region; then, the dynamic segmentation is implemented to determine non-acceptable segments along the pipeline abscissa; and finally, the groups with the greater failure probability are located in those segments.

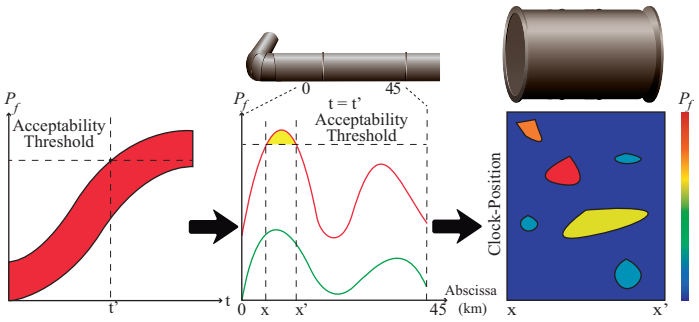

Figure 3: Pipeline Integrity Evaluation Approach.

Additionally, a cost evaluation is carried out using the maintenance and failure unit costs reported by Zhang & Zhou (2014). These costs depend on the number of the intervened joints, so this number is estimated using the cumulative non-acceptable segment (according to DNV) of the pipeline and an equivalent distance of the pipe joint. Overall, two main costs are considered: i) A maintenance costs from ILI inspections, pipeline excavations, and coating reinforcements of $72,902.57 USD/Joint, and ii) Direct costs due to a failure costs of $105,221.87 USD/Joint. Algorithm 3 describes the procedure for this method.

3. Case Study

The case study consists of a carbon steel pipeline grade API5LX52 alloy with the characteristics shown in Table 3. Two corrosion data sets were obtained from ILI measurements 2 years apart. In the first run, 33,466 defects were identified and in the second 59,101 out of which almost 50% were associated with pitting corrosion, and the remaining are distributed mainly in circumferential slotting. The defects are mostly at the inner wall (around 80%) in both measurements.

Algorithm 3 Critical pipeline segments identification and evaluation

Input: T (Evaluating years), data to determine the combined Failure Probability (See Section 2.2), maintenance (m) and failure (f) unit costs, a safety acceptable criterion C, and a joint length δ.

Procedure: Pipeline critical segments & Maintenance($\mathcal{M}$)/Failure ($\mathcal{F}$)Costs

1: Determine the corrosion groups and their equivalent dimensions {See Section 2.3.1}
2: $\mathcal{L} = 0$ {$\mathcal{L}$: Non-acceptable length segments}
3: **for** $t = 1$ to T **do**
4: Determine the Combined P_f {See the Algorithm 1}.
5: Determine the Dynamic Segmentation and the Critical Region {See Section 2.2.4}.
6: Find the segments $\mathcal{N}$ such that $\mathcal{E}_L \geq C$ {$\mathcal{E}_L$ the lower envelope}
7: $\mathcal{L} \leftarrow \mathcal{L} + \mathcal{N}$.
8: **end for**
9: Calculate $\mathcal{M} = m\frac{\mathcal{L}}{\delta}$ and $\mathcal{F} = f\frac{\mathcal{L}}{\delta}$

Table 3: Case study main parameters

Parameter	Value	Units
Outer diameter	273.1	mm
Nominal diameter	10	in
Pipeline length	44	km
MAOP (Maximum Allowable Operating Pressure)	1500	psig
SMYS (Specified Minimum Yield Strength)	52,000	psig
SMTS (Specified minimum tensile strength)	60,000	psig
Average wall thickness	6.35	mm
Operating temperature range	303.55-307.05	K
Operating velocity range	1.7-2.4	m/s

4. Results and discussion

4.1. Data treatment

Increments obtained from two ILI measurements were used to calibrate the stochastic process assuming independence between the defects and their depths. Because the exact MFL tool used to inspect the pipeline was not known, a circumferential uncertainty of 5°during the inspection was assumed based on the vendor technical reports as it was described in Amaya-Gómez et al. (2016). This uncertainty corresponds to 12 mm or a deviation of 5%, which is used to obtain two different data sets i) defects with a depth change between the two ILI measurements at the same position, and ii) defects located between the ILI measurements with a deviation less or equal than 5%. These sets were used to determine the growth corrosion model based on the defects reported from both ILI measurements at the inner wall; defects with no correspondence between the two ILI measurements were discarded (Amaya-Gómez et al., 2018). This degradation model was later applied to the defects in the last inspection.

4.2. Combined Failure Probability

Some considerations are in place to calculate the pressure and stress failure probabilities. For the energy distortion model (stress failure criterion), the tensile strength was implemented instead of the yield strength to be consistent with the fracture of the material like in the case of the burst pressure. The parameters of each approach were obtained from the ILI measurements of the case study or by the following considerations:

- The operating pressure was assumed to follow a Gumbel distribution following the recommendations of CSA (2007). The parameters for this distribution were obtained from the method discussed by Hasan et al. (2012).

- Defects depth for the first year were obtained from the last ILI measurement. The remain depths were determined from the Mixed Lévy degradation mechanism with Gamma and CPP-Delta processes (See Amaya-Gómez et al. (2018)).

- The trench width in which the pipeline is buried was assumed to be 26 inches (660 mm), following the reported by McAllister (2014) for a nominal pipeline of 10 inches.

- The remaining pipeline properties were: i) the elasticity module of API5L X52 grade carbon steel of 210,000 MPa (TMI, 2011), ii) the Poisson coefficient of 0.3 (Bokaian, 2004), and iii) the thermal expansion coefficient of $11.7x10^{-6}$ /°C (Ahammed & Melchers, 1997; Bokaian, 2004).

- The soil load was determined using an equivalent volume of the buried pipeline. This volume was calculated using the buried dimensions for a nominal diameter of 10 inches (Gulf Interstate Engineering, 1999). Then, the unitary weight reported by Ahammed & Melchers (1997) was implemented to obtain a soil load of 228 kN.

- The soil properties were taken from Ahammed & Melchers (1997). Their distributions were assumed to be normal except for C_t, k_d and k_m, which were represented by lognormal distributions. Additionally, L_e, B_d, C_d, E, F, r, α, γ, μ and $\Delta\theta$ were assumed to be constant, following the suggestions of these authors.

Based on these considerations, the failure probability for the combined, pressure and stress failure probabilities were determined (Fig. 4). For the first 5 years, the differences between the three failure probabilities are imperceptible, but after the 10th year, the pressure failure results differ appreciably from the stress predictions (obtaining a difference near 0.2). Regarding the combined and stress results, their results vary only 1% indicating that practically each failure state in the pressure criterion is also a failure state in the stress criterion.

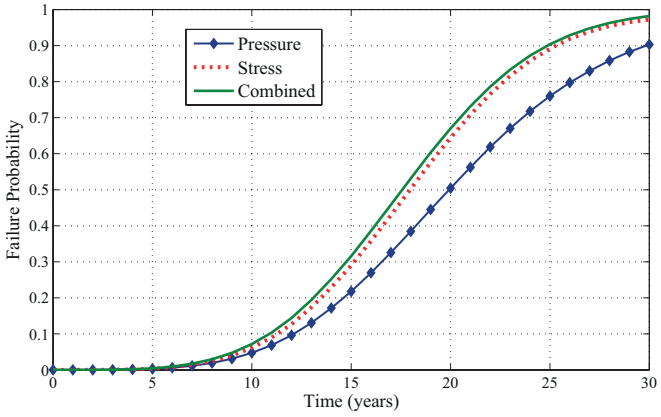

Figure 4: Combined Pressure-Stress Failure Probability.

4.3. Dynamic Segmentation and Critical Region

The following parameters for the dynamic segmentation were considered based on the reported joints: $\underline{\delta} = 5$, $\overline{\delta} = 100$, and $\Delta d_{seg} = 1$. Fig 5 illustrates the results obtained following Algorithm 2 for 40 years. The y-axis corresponds with the time evaluated, the x-axis with the assessed static segment length within $[\underline{\delta}, \overline{\delta}]$, and the color represents the indicator results from Eq. 7 (see Algorithm 2). The greater results of this indicator were located from 5 to 30 years, whereas for the first 5 years and after the 30th year the results were less than 5%. This result suggests that the failure probabilities of both envelopes are close to the obtained result without segmentation; thus, the required length does not differ drastically with the fixed approach. Interestingly, the greater differences were found in a segment length between 10 to 15 meters; a segment length that matches with the case study joint length range (almost 78% are between 10 and 14 meters). These results would suggest that a great focus of corrosion defects are located near the pipeline joints, which according to Dzioyev et al. (2014) are commonly found 200 mm from the welding unions.

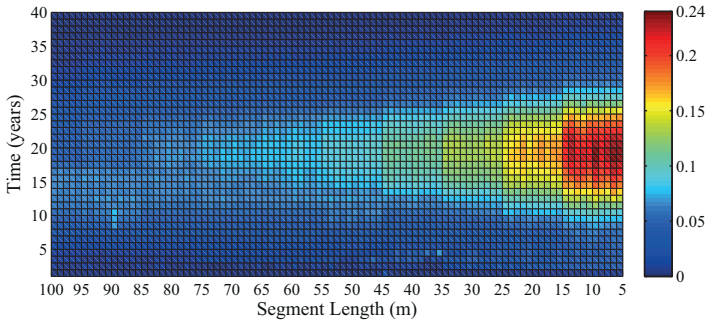

Figure 5: Sensitivity Results for the segmentation distance.

To illustrate how this approach identifies critical zones along the pipeline, a dynamic segmentation at 10 years using $d_{seg} = 9$ meters was obtained and depicted in Fig. 6. This figure shows the failure probability without segmentation $P_{f_{NS}}$ around 0.04, the upper envelope as the dashed line, and the lower envelope as the solid line. The results for this illustrative example show that significant differences were obtained between the two envelopes with $P_{f_{NS}}$ in 0-5 km and 25-30 km. Note also that the lower envelope surpasses $P_{f_{NS}}$ near 4 km, which demonstrates that the spatial variability is certainly a matter of concern for pipeline reliability analysis.

Finally, the critical region was defined to evaluate pipeline condition over time. Quartiles of the envelopes were used to generate three critical regions depending on the concentration of data: i) 25%, ii) 50%, and iii) 75% (Fig. 7). These critical regions expose an important variability throughout the pipeline obtaining ranges near two orders of magnitude, so their selection is supported against an approach without any segmentation. Additionally, this figure indicates that the main differences between the envelopes with the $P_{f_{NS}}$ are in the range of 5-30 years, as in the case of Fig. 5.

The proposed critical region is an interesting alternative to integrity evaluations that are commonly based on fixed segmentations (Dawotola et al., 2011; Hallen et al., 2003). This approach follows a continuous-reliability assessment based on a corrosion degradation process that can be used with acceptability thresholds to support decision-making in future interventions. For instance, if the DNV RP-F101 Low Safety Level ($< 10^{-3}$) is implemented, an intervention can

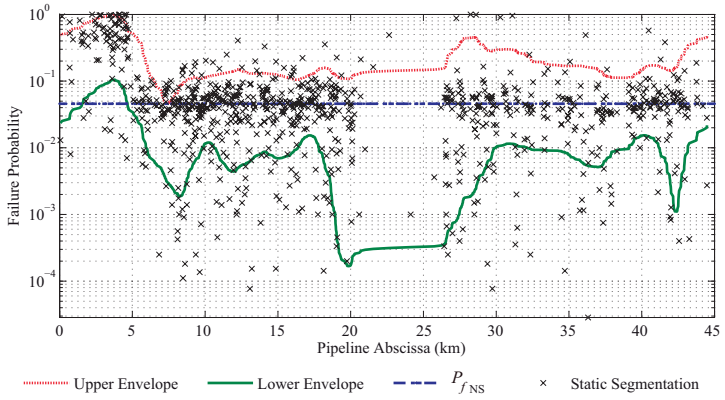

Figure 6: Dynamic Segmentation Results for 10 years and $d_{seg} = 9$.

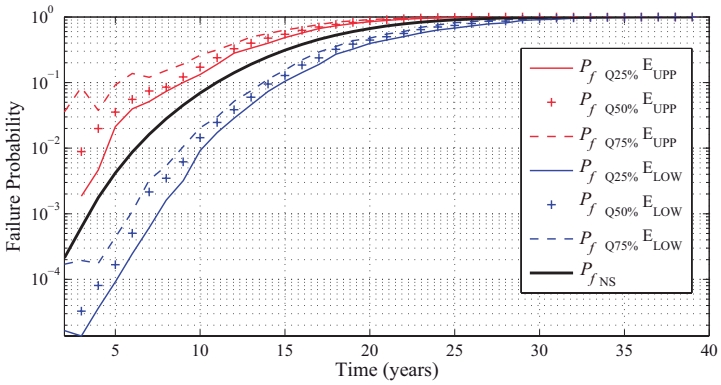

Figure 7: Critical Region Results.

be recommended in the next 6-7 years because the lower envelope exceeds this threshold. This approach can be used with other spatial evaluations including soil aggressiveness (Sahraoui & Chateauneuf, 2016) and population density to support a risk-based assessment.

4.4. Grouping criteria evaluation

The ILI report provides a list of clusters (potential "corrosion colonies") and a groupable classification of every defect from which these groups are created. Nevertheless, from the 47,663 groupable defects reported on the last ILI measurement, only 18,276 were assigned to one of the 6538 corrosion groups. Then, these corrosion groups were used as a training set and the defects without a group as a test set for supervised learning. Unsupervised learning was developed using all the groupable defects.

The grouping alternatives were compared based on their main capabilities to capture corrosion adjacent defects. Table 4 compares the number of groups obtained, the average number of defects per group, and the total grouped defects. Despite the ASME approach have the highest number of groups, the number of defects per group is not significant in comparison to an individual assessment. Moreover, this approach uses only 44% of the groupable defects on the inner

wall, which may not affect the reliability from the case of isolate defects. These results illustrate that the ASME B31G approach does not capture all the possible corrosion groups (colonies); hence, it underestimates the pipeline condition.

Table 4: Summary of the results of the grouping approaches evaluated.

Grouping criterion	API 579	ASME B31G	DNV RP-F101	KNN+KM	KM
Number of obtained groups	3,106	8,263	5,466	8,085	8,000
Mean number of defects by group	15	3	9	7	6
Total grouped defects	46,536	24,176	44,890	48,338	43,399

For the remaining standards criteria, their grouping capabilities follow similar performances. API 579 criterion has a higher number of defect per group based on the mean number of defects and the ratio between the groups with the grouped defects. The latter because 502 records in the last ILI run reported a length greater than 1 meter, which bearing in mind that this criterion is based on the length and the width, would obtain an important amount of clustering defects. Nevertheless, this approach tends to be conservative because the 502 defects do not report a significant depth. DNV RP-F101 approach also has a high amount of defects per group because of its limit distance in the circumferential direction. However, this criterion has a homogeneous behavior on the pipeline that is evidenced in the higher number of groups. The synthetic learning approaches follow a correlated performance, which is evidenced in all the parameters reported in Table 4. For a deeper comparison among these alternatives, corrosion groups distribution were determined for each alternative obtaining the contours depicted in Fig. 8.

This figure confirms that ASME B31G is not an adequate grouping criterion for corrosion defects. This grouping criterion lacks many corrosion defects per cluster in comparison to the other alternatives. For instance, near 18 km this approach report 200 defects and the other grouping approaches a defect density near to 300. These criteria are based exclusively on the location and proximity with their neighbors, so the non-inclusion of a defect with a significant depth may underestimate pipeline risk. Regarding the other alternatives, they did not present significant variations in their groups' distribution although they follow a different construction and evaluation criteria. They implement almost the same proportion of defects, which suggest that these alternatives can represent an interesting possibility in a corrosion colony evaluation.

Finally, the reliability effect of these grouping criteria was compared against isolated defects by their mean failure probabilities (see Algorithm 1). The obtained results –shown in Fig. 9– agree with the previous statement about ASME B31G criterion. Its failure probability does not differ significantly from the corresponding for individual defects, which underestimates the pipeline condition in case defects are assessed isolated. The other alternatives show important differences with isolated defects. For instance, the two synthetic approaches increase almost 10% in their failure probability during 12-18 years from the individual defects. The results for these two approaches match almost entirely, except for an initial time-span in which the KNN+KM approach was slightly higher. The results of DNV RP-F101 and API 579 approaches follow expected behaviors based on the discussion mentioned above.

The above results suggest that the standards approaches could represent conservative grouping alternatives in comparison to the synthetic learning techniques. Indeed, ASME B31G grouping criterion is a non-suitable alternative for grouping corrosion defects since it does not describe all possible corrosion groups. API 579 approach is a conservative alternative because of the possibility of corrosion defects with considerable lengths and lower depths. DNV RP-F101 alternative gives conservative results related to their circumferential limit, but it represents an interesting

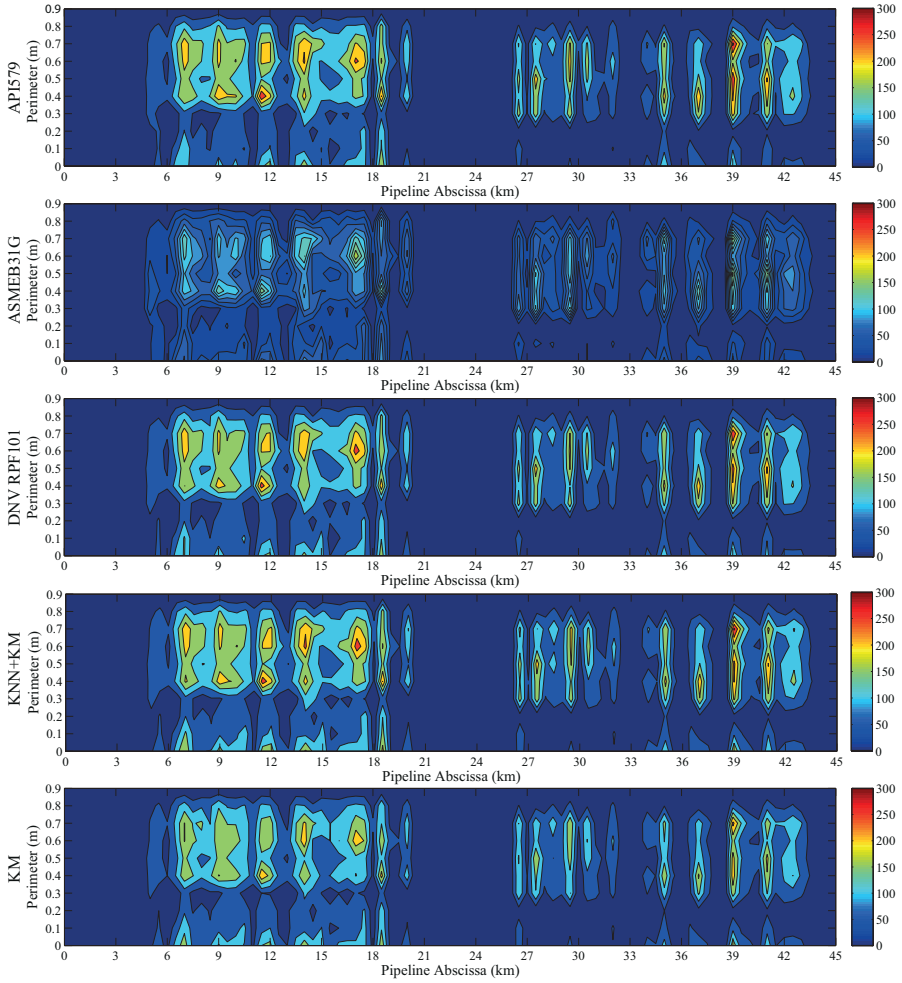

Figure 8: Grouped defects contours based on the grouping criteria.

corrosion grouping possibility due to its difference with the synthetic learning approaches.

4.5. Pipeline Integrity evaluation approach

To illustrate the proposed approach, the DNV RP-F101 grouping criterion was implemented to evaluate possible clusters along the pipeline. The DNV Low Safety threshold $C = 10^{-3}$ was also considered to discriminate non-acceptable segments based on the lower envelope with 75% of data. The results depicted in Fig. 10 show that non-acceptable segments begin around the fifth year. Then, the dynamic segmentation for this evaluating year reveals that the non-acceptable segments would be in the first six kilometers and the range of 40-45 km. Finally, considering the corrosion defects location, two defects with higher failure probability were identified at km 5066.

Regarding the cost evaluation, recall that $f = \$105,221.87$ USD/ Joint and $m = \$72,902.57$ USD/ Joint were used as input data in Algorithm 3. For comparison purposes, the three DNV

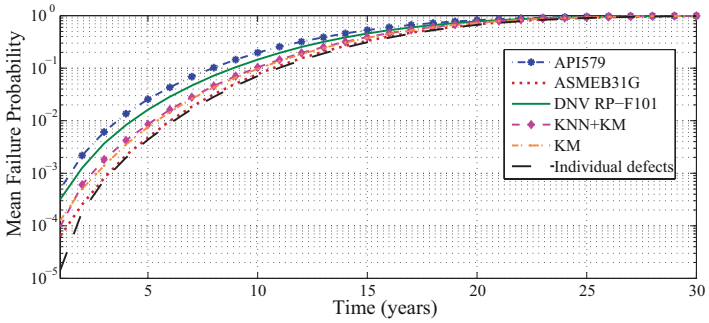

Figure 9: Failure Probability results using grouping criteria.

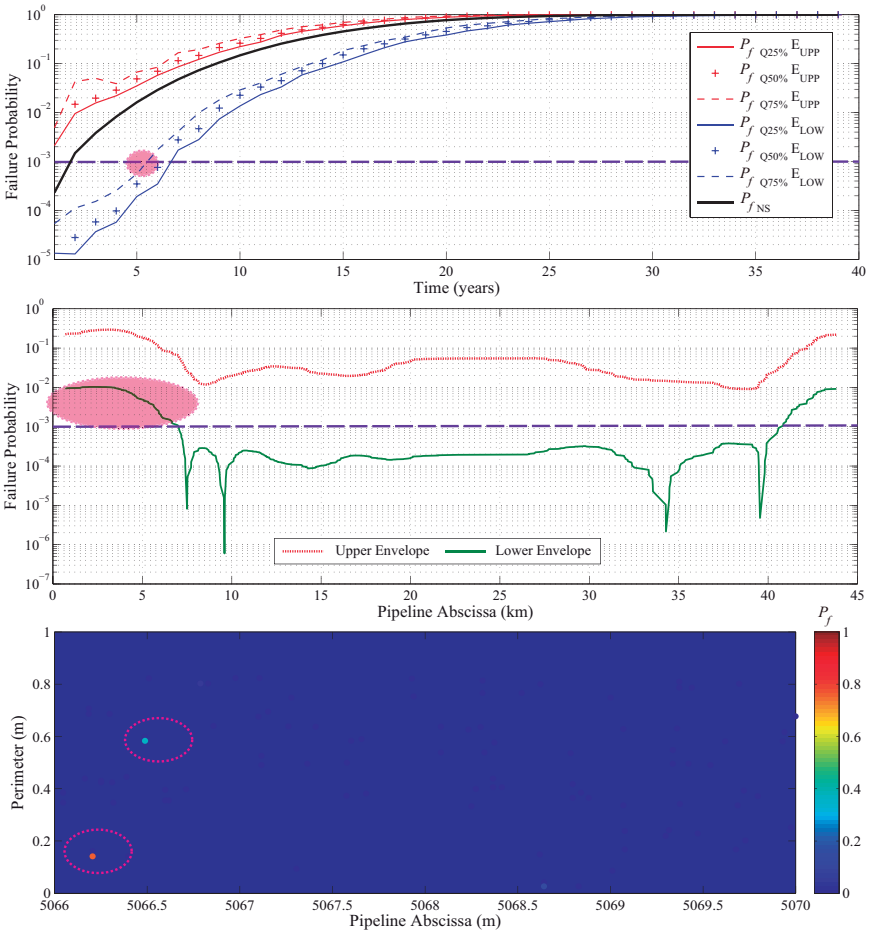

Figure 10: Pipeline Integrity Evaluation Results for the case of study with the DNV grouping criterion.

safety thresholds were considered; i.e., $C_1 = 10^{-1}$, $C_2 = 10^{-2}$, and $C_3 = 10^{-3}$. Fig. 11 shows the accumulate non-acceptable segments using these three criteria. The results show that in 10 years the length of the pipeline that requires intervention with a threshold of C_3 is about 40 km, with C_2 is 15 km, and for C_1 less than 8 km. Moreover, for the first 15 years, the pipeline would be compromised since half of its abscissa achieved a failure probability higher than 10^{-1}.

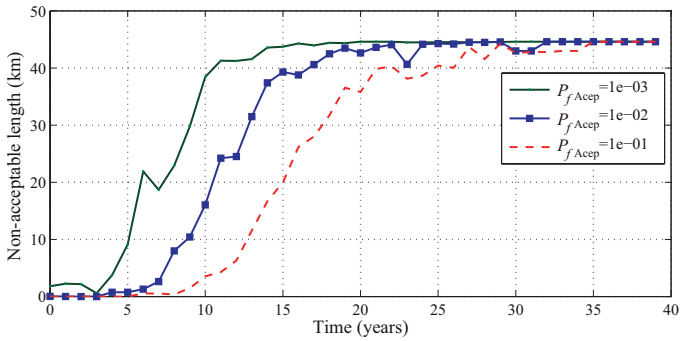

Figure 11: Accumulate non-acceptable pipeline segments.

The corresponding maintenance and failure costs are determined for a system without any intervention using a continuous discounted rate of 5%, a mean joint length of 12 m, and the accumulate non-acceptable segments obtained before with $C = 10^{-1}$ (Fig. 12). The results allow decision-makers to evaluate future interventions along the pipeline. For instance, this figure suggests that for the first 5 years the system failure investment would be similar than for required maintenance; however, after the 10th year, the required investment in case of a failure is 20 Million USD greater than if maintenance is implemented.

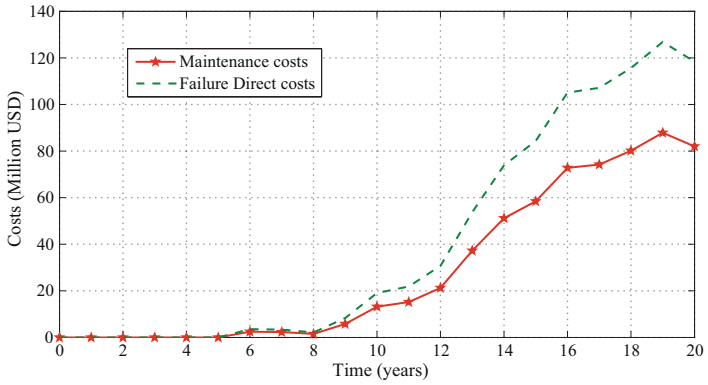

Figure 12: Maintenance and failure discounted costs with $C = 10^{-1}$.

This work proposes an alternative integrity evaluation considering the spatial distribution of defects and the formation of "corrosion colonies" along the pipeline; nevertheless, in this work, we do not contemplate the effect of the surrounding environment (e.g., soil) on the degradation process. However, it has to be recognized the role played by the soil in pipeline degradation (i.e., metal loss) in the form of external corrosion (Castaneda & Rosas, 2015). A complete integrity

evaluation should include a space-dependent degradation process caused by defects located at the outer wall. In this direction, some interesting approaches have been proposed such as the one reported by Sahraoui & Chateauneuf (2016), which used a Gaussian random field based on the Karhunen-Loève expansion depending on the type of soil. Wang and co-workers have developed a framework that cluster defects depending on their corrosion rates, which are later used with Monte Carlo simulations and Markov Chains to estimate a space-dependent corrosion rate probability density (Wang et al., 2015b). This approach uses a Gaussian mixture model (GMM) clustering criterion due to better separability capabilities in comparison to a K-means approach (Yajima et al., 2015).

5. Conclusions

An integrity evaluation was proposed for corroded pipelines based on a critical region and a dynamic segmentation. The proposed approach can identify critical segments temporally and spatially along the pipeline lifetime that can support future intervention decisions. The dynamic segmentation was developed from upper and lower envelopes from a set of shifted static segmentations. The critical region was determined based on the dynamic segmentation results quartiles. In both cases, a pressure-stress combined failure probability and a grouping evaluation of corrosion defects were considered.

For the corrosion grouping, three limit distance approaches (i.e., API 579, ASME B31G, and DNV RP-F101) and two synthetic learning approaches (i.e., KNN+KM and KM) were compared based on their obtained groups distribution and their failure probability against isolated defects. ASME B31G criterion was a non-suitable alternative because the information captured do not represent the real state of the system. API 579 approach represents a conservative alternative in case defects have important lengths. DNV RP-F101 criterion was conservative because of their limit circumferential distance, but it represents an interesting alternative due to its similarity with the synthetic learning approaches.

The proposed approach allows decision makers to identify critical segments temporally and spatially along the pipeline based on acceptable thresholds as the one reported by DNV RP-F101. Based on a real case study, it was possible to identify that during the first five years interventions should be focus near the fifth kilometer.

Acknowledgments

R. Amaya-Gómez thanks the National Department of Science, Technology and Innovation of Colombia for the PhD scholarship (COLCIENCIAS Grant No. 727, 2015).

Bibliography

Adib-Ramezani, H., Jeong, J., & Pluvinage, G. (2006). Structural integrity evaluation of X52 gas pipes subjected to external corrosion defects using the SINTAP procedure. *International Journal of Pressure Vessels and Piping*, *83*, 420 – 432. doi:http://dx.doi.org/10.1016/j.ijpvp.2006.02.023.

Ahammed, M., & Melchers, R. (1997). Probabilistic analysis of underground pipelines subject to combined stresses and corrosion. *Engineering Structures*, *19*, 988 – 994. doi:http://dx.doi.org/10.1016/S0141-0296(97)00043-6.

Amaya-Gómez, R., Riascos-Ochoa, J., Muñoz, F., Bastidas-Arteaga, E., Schoefs, F., & Sánchez-Silva, M. (2018). Modeling of pipeline corrosion degradation mechanism with a Lévy Process based on ILI (In-Line) Inspections, . Under second review.

Amaya-Gómez, R., Sánchez-Silva, M., Bastidas-Arteaga, E., Schoefs, F., & Muñoz, F. (2019). Reliability assessments of corroded pipelines based on internal pressure A review. *Engineering Failure Analysis*, . doi:https://doi.org/10.1016/j.engfailanal.2019.01.064.

Amaya-Gómez, R., Sánchez-Silva, M., & Muñoz, F. (2016). Pattern recognition techniques implementation on data from In-Line Inspection (ILI). *Journal of Loss Prevention in the Process Industries*, *44*, 735 – 747. doi:http://dx.doi.org/10.1016/j.jlp.2016.07.020.

Amirat, A., Chaoui, K., Azari, Z., & Pluvinage, G. (2004). Residual stress analysis in seamless APIX60 Steel Gas Pipelines. *Revue Sciences et Technologie, de l'Université Mentouri de Constantine*, (pp. 7 – 14).

Amirat, A., Mohamed-Chateauneuf, A., & Chaoui, K. (2006). Reliability assessment of underground pipelines under the combined effect of active corrosion and residual stress. *International Journal of Pressure Vessels and Piping*, *83*, 107 – 117. doi:http://dx.doi.org/10.1016/j.ijpvp.2005.11.004.

Andrade, E., & Benjamin, A. (2004). Structural Evaluation of Corrosion Defects in Pipelines: Comparison of FE Analyses and Assessment Methods. In *Proceedings of the Fourteenth International Offshore and Polar Engineering Conference* (pp. 120–126). Toulon, France.

API (2007). *API 579-1/ASME FFS-1*. Technical Report American Petroleum Institute Washington, USA.

ASME (2009). *ASMEB31G: Manual for determining the remaining strength of corroded pipelines*. Technical Report American Society of Mechanical Engineers.

Benjamin, A., Freire, J., & Vieira, R. (2007). Part 6: Analysis of pipeline containing interacting corrosion defects. *Experimental Techniques*, *31*, 74–82. doi:10.1111/j.1747-1567.2007.00190.x.

Benjamin, A., Freire, J., Vieira, R., & Cunha, D. (2016). Interaction of corrosion defects in pipelines Part 1: Fundamentals. *International Journal of Pressure Vessels and Piping*, *144*, 56 – 62. doi:https://doi.org/10.1016/j.ijpvp.2016.05.007.

Berstad, T., Dørum, C., Jakobsen, J., Kragset, S., Li, H., Lund, H., Morin, A., Munkejord, S., Mølnvik, M., Nordhagen, H., & Østbya, E. (2011). {CO2} pipeline integrity: A new evaluation methodology. *Energy Procedia*, *4*, 3000 – 3007. doi:http://dx.doi.org/10.1016/j.egypro.2011.02.210. 10th International Conference on Greenhouse Gas Control Technologies.

Bokaian, A. (2004). Thermal expansion of pipe-in-pipe systems. *Marine Structures*, *17*, 475 – 500. doi:http://dx.doi.org/10.1016/j.marstruc.2004.12.002.

Caleyo, F., Velázquez, J., Valor, A., & Hallen, J. (2009). Probability distribution of pitting corrosion depth and rate in underground pipelines: A Monte Carlo study. *Corrosion Science*, *51*, 1925 – 1934. doi:http://dx.doi.org/10.1016/j.corsci.2009.05.019.

Castaneda, H., & Rosas, O. (2015). External Corrosion of Pipelines in Soil. In *Oil and Gas Pipelines* chapter 20. (pp. 265–274). John Wiley & Sons, Ltd. doi:10.1002/9781119019213.ch20.

CSA (2007). *CSA Z662-07: Limit state equation for burst of large leaks and rupture for corrosion defect*. Technical Report Canadian Standard Association.

Dawotola, A., van Gelder, P., Charima, J., & Vrijling, J. (2011). Applications of Statistics and Probability in Civil Engineering. chapter Estimation of failure rates of crude product pipelines. CRC Press.

de Waard, C., & Lotz, U. (1993). Prediction of CO2 corrosion of carbon steel. In *NACE International*. Houston, United States.

DNV (2010). *DNV-RP-F101: Recommended practice. Corroded Pipelines*. Technical Report Det Norske Veritas Høvik, Norway.

Dzioyev, K., Basiyev, K., Khabalov, G., & Dzarukayev, E. (2014). Stress corrosion processes in the metal and welded joints in gas pipelines. *Welding International*, *28*, 717–721. doi:10.1080/09507116.2013.852335.

ERCB (2011). *Directive 066: Requirements and Procedures for Pipelines*. Technical Report Energy Resources Conservation Board Calgary, Alberta, Canada.

Garcia, D. (2014). Matlab File Exchange: SMOOTH1Q. https://www.mathworks.com/matlabcentral/fileexchange/37878-quick---easy-smoothing.

Gomes, W., & Beck, A. (2014). Optimal inspection and design of onshore pipelines under external corrosion process. *Structural Safety*, *47*, 48 – 58. doi:http://dx.doi.org/10.1016/j.strusafe.2013.11.001.

Gulf Interstate Engineering (1999). *Temporary Right-of-Way Width Requirements for Pipeline Construction*. Technical Report The INGAA Foundation. Inc. URL: http://mrsc.org/getmedia/8B8FF358-4055-4D0E-9ED6-08AE41DA68B7/EiberOverview.aspx.

Hallen, J., Caleyo, F., & González, J. (2003). Probabilistic Condition Assessment of Corroding Pipelines in Mexico. In *III Pan-American Conference for Nondestructive Testing*. Rio de Janeiro, Brasil.

Hasan, S., Khan, F., & Kenny, S. (2012). Probability assessment of burst limit state due to internal corrosion. *International Journal of Pressure Vessels and Piping*, *89*, 48 – 58. doi:http://dx.doi.org/10.1016/j.ijpvp.2011.09.005.

Kale, A., Thacker, B., Sridhar, N., & Waldhart, J. (2004). A probabilistic model for internal corrosion of gas pipeline. In *2004 International Pipeline Conference*. Alberta, Canada.

Kishawy, H. A., & Gabbar, H. A. (2010). Review of pipeline integrity management practices. *International Journal of Pressure Vessels and Piping*, *87*, 373 – 380. doi:http://dx.doi.org/10.1016/j.ijpvp.2010.04.003.

Li, S., Yu, S., Zeng, H., Li, J., & Liang, R. (2009). Predicting corrosion remaining life of underground pipelines with a mechanically-based probabilistic model. *Journal of Petroleum Science and Engineering*, *65*, 162 – 166. doi:http://dx.doi.org/10.1016/j.petrol.2008.12.023.

Martin, A. (2010). Matlab File Exchange: env secant. https://www.mathworks.com/matlabcentral/fileexchange/27662-env-secant-x-data--y-data--view--side-.

McAllister, E. (2014). *Pipeline Rules of Thumb Handbook: A Manual of Quick, Accurate Solutions to Everyday Pipeline Engineering Problems*. Elsevier Science.

Muhlbauer, W. (2004). *Pipeline Risk Management Manual: Ideas, Techniques, and Resources*. Elsevier Science.

NACE International (2002). *RP0502-2002 Pipeline External Corrosion Direct Assessment Methodology. Standard Recommended Practice*. Technical Report Houston,USA.

Netto, T., Ferraz, U., & Estefen, S. (2005). The effect of corrosion defects on the burst pressure of pipelines. *Journal of Constructional Steel Research*, *61*, 1185 – 1204. doi:http://dx.doi.org/10.1016/j.jcsr.2005.02.010. Second Brazilian special issue.

NORSOK (1998). *CO2 corrosion rate calculation model*. Technical Report Oslo, Norway.

Pandey, M., & Lu, D. (2013). Estimation of parameters of degradation growth rate distribution from noisy measurement data. *Structural Safety*, *43*, 60 – 69. doi:http://dx.doi.org/10.1016/j.strusafe.2013.02.002.

Sahraoui, Y., & Chateauneuf, A. (2016). The effects of spatial variability of the aggressiveness of soil on system reliability of corroding underground pipelines. *International Journal of Pressure Vessels and Piping*, *146*, 188 – 197. doi:http://dx.doi.org/10.1016/j.ijpvp.2016.09.004.

Sahraoui, Y., Khelif, R., & Chateauneuf, A. (2013). Maintenance planning under imperfect inspections of corroded pipelines. *International Journal of Pressure Vessels and Piping*, *104*, 76 – 82. doi:http://dx.doi.org/10.1016/j.ijpvp.2013.01.009.

Sánchez-Silva, M., & Klutke, G.-A. (2016). *Reliability and life-cycle analysis of deteriorating systems*. Springer series in Reliability Engineering. Springer.

Tang, P., Yang, J., Zheng, J., Wong, I., He, S., Ye, J., & Ou, G. (2009). Failure analysis and prediction of pipes due to the interaction between multiphase flow and structure. *Engineering Failure Analysis*, *16*, 1749 – 1756. doi:http://dx.doi.org/10.1016/j.engfailanal.2009.01.002.

Teixeira, A., Guedes Soares, C., Netto, T., & Estefen, S. (2008). Reliability of pipelines with corrosion defects. *International Journal of Pressure Vessels and Piping*, *85*, 228 – 237. doi:http://dx.doi.org/10.1016/j.ijpvp.2007.09.002.

TMI (2011). *Steel pipes for pipelines for combustible fluids*. Technical Report ThyssenKrupp Materials International Washington, USA. URL: http://www.s-k-h.com/media/de/Service/Werkstoffblaetter_englisch/Leitungsrohre/X52_L360xx_engl.pdf material data sheet X52.

Varga, L., & Fekete, G. (2017). Continuous integrity evaluation of corroded pipelines using complemented FEA results - Part I: Procedure development. *International Journal of Pressure Vessels and Piping*, *150*, 19 – 32. doi:http://dx.doi.org/10.1016/j.ijpvp.2016.12.010.

Wang, H., Yajima, A., Liang, R., & Castaneda, H. (2015a). A Bayesian model framework for calibrating ultrasonic in-line inspection data and estimating actual external corrosion depth in buried pipeline utilizing a clustering technique. *Structural Safety*, *54*, 19 – 31.

Wang, H., Yajima, A., Liang*, R. Y., & Castaneda, H. (2015b). Bayesian Modeling of External Corrosion in Underground Pipelines Based on the Integration of Markov Chain Monte Carlo Techniques and Clustered Inspection Data. *Computer-Aided Civil and Infrastructure Engineering*, *30*, 300–316. doi:10.1111/mice.12096.

Yajima, A., Wang, H., Liang, R., & Castaneda, H. (2015). A clustering based method to evaluate soil corrosivity for pipeline external integrity management. *International Journal of Pressure Vessels and Piping*, *126-127*, 37 – 47. doi:https://doi.org/10.1016/j.ijpvp.2014.12.004.

Zhang, G., Zeng, L., Huang, H., & Guo, X. (2013). A study of flow accelerated corrosion at elbow of carbon steel pipeline by array electrode and computational fluid dynamics simulation. *Corrosion Science*, *77*, 334 – 341. doi:http://dx.doi.org/10.1016/j.corsci.2013.08.022.

Zhang, S., & Zhou, W. (2014). Cost-based optimal maintenance decisions for corroding natural gas pipelines based on stochastic degradation models. *Engineering Structures*, *74*, 74 – 85. doi:http://dx.doi.org/10.1016/j.engstruct.2014.05.018.